Image-based Material Characterization for Daylight Simulation Using Illuminance-proxy and Artificial Neural Networks

Forouzandeh Shahraki, N.; Brembilla, E.; Jakubiec, John Alstan

Publication date
2022

Document Version
Final published version

Published in
Proceedings of the 14th European Lighting Conference LUX EUROPA 2022

Citation (APA)
Forouzandeh Shahraki, N., Brembilla, E., & Jakubiec, J. A. (2022). Image-based Material Characterization for Daylight Simulation Using Illuminance-proxy and Artificial Neural Networks. In *Proceedings of the 14th European Lighting Conference LUX EUROPA 2022* (pp. 171-178).

Image-based Material Characterization for Daylight Simulation Using Illuminance-proxy and Artificial Neural Networks

Nima Forouzandeh
Faculty of Architecture & the Built Environment
Delft University of Technology
Delft, Netherlands
ORCID: 0000-0001-7025-5509

Eleonora Brembilla
Faculty of Architecture & the Built Environment
Delft University of Technology
Delft, Netherlands
ORCID: 0000-0003-1800-8660

J. Alstan Jakubiec
John H. Daniels Faculty of Architecture, Landscape and Design
University of Toronto
Toronto, Canada
ORCID: 0000-0002-8534-6902

***Abstract*—A key aspect of daylight modeling is the definition of material optical properties. Characterization of such properties in existing indoor spaces with current methods is a labour-intensive and time-consuming task, especially in surfaces with considerable visual complexity. Faster and more accurate estimations of such properties will lead to more efficient workflows. Towards this direction, the present work studied the feasibility of using two novel approaches i.e. illuminance-proxy and probabilistic image based material characterization methods for implementation in daylight modeling. These approaches are compared with two common techniques, namely the manual selection from a measured dataset and the use of illuminance/luminance measurements. According to the results, both novel techniques are able to predict spatially-averaged Daylight Autonomy, continuous Daylight Autonomy, and Useful Daylight Illuminance in 300-3000 lx range with less than 5% error.**

***Keywords*—on-site, field, measurement, visual, Digitalization, Optical.**

I. Introduction

Sufficient and proper daylight in indoor spaces lead to more energy-efficient buildings and has a significant impact on users' satisfaction and well-being[1, 2].

Numerical simulation of daylight has been extensively implemented in recent decades as a reliable tool to assess the performance of buildings for improving existing indoor spaces and designing future buildings. Such a numerical model is not only applied for design and retrofit purposes, but it is also capable of acting as a virtual representation of a building which can potentially be applied for making several kinds of real-time to long-term decisions during the building life-cycle. The key to constructing this so-called "digital twin" is, on one hand, dependent upon the calculation and estimation algorithms, and on the other hand, accurate and reliable inputs, based on which making such informed decisions will be feasible.

As far as daylight is concerned, the optical properties of different surfaces within an indoor space are important determinants of its short-term and long-term performance[3]. While this information can be defined roughly according to design specifications in the pre-construction phases, measurements are, in most cases, necessary for creating an accurate model. With current methods, however, this demands a considerable on-site field measurement effort followed by manual modeling, which makes daylight analyses costly for many applications and real-time decision-making impossible.

To tackle these limitations, two image-based techniques for pixel-wise and patch-wise material characterization are tested in estimation of material properties in a real indoor space. These results are then implemented for daylight simulation and calculation of annual performance.

II. Background

A. Illuminance-proxy method

Characterization of dense, pixel-wise reflectance maps of arbitrarily complex diffuse surfaces using High Dynamic Range Imaging (HDRI) has been studied by Mardaljevic, Brembilla, and Drosou [4], [5]. This approach derives an illuminance map, based on interpolation of sparsely known reflectance values on a surface. Since it requires only a few known reflectance values on a surface, this method can reduce the field measurement labor, while giving a pixel-wise reflectance map.

B. Probabilistic material characterization

The existing body of literature on probabilistic material characterization in computer vision attempts to minimize the measurement cost by probabilistic characterization of material optical properties. This is done with the help of supervised learning algorithms, mainly Convolutional Neural

Networks (CNN) trained with labeled datasets of materials. These datasets can be categorized according to acquisition method, including real-world images (e.g., MINC[6] and OpenSurfaces[7]), synthesized sets of images, and measured datasets (e.g., BTF material database[8] and SVBRDF database Bonn[9]). Another example of measured datasets, relevant to the daylighting field, is Spectral Materials Database (SpectralDB), a work done by Jakubiec [10]. This is extensively used by daylight modellers and researchers to define materials in simulation models for evaluation of daylight provision, visual comfort and non-visual effects of light on building occupants. However, the applicability of this dataset for image-based probabilistic estimation of key material information for daylight simulation (i.e., $\text{reflectance}_{\text{RGB}}$, specularity, and roughness) is not yet studied, which is one of the objectives of the present work.

III. Objectives

This study investigates the feasibility of using the illuminance-proxy method as an efficient characterization approach for pixel-wise reflectance calculation for modeling daylight in existing indoor spaces.
Moreover, it aims to study the feasibility of using a learning-based approach for estimating material optical properties with only a small-size (128*128 pixels) rectangular RGB patch from an image taken with a regular camera. This is an effort towards automation of daylight modeling in existing indoor spaces, and to address the lack of coordination with other related fields, such as geomatics and scan-to-BIM [11].

IV. Methods

Four material characterization scenarios are considered for the purpose of this study, each applied to the same daylight model of a case study room.
The results of annual daylight simulations obtained using these methods are then compared and discussed. The following subsections describe the case study room, simulation parameters, material characterization scenarios, and data analysis methods.

A. The case study room

The studied room is a 5.8 m by 4.3 m meeting room located at the Faculty of Architecture in Delft, The Netherlands. The room is oriented towards South-East with a 4 degrees angle from due South. Pictures from the room are presented in Fig. 1

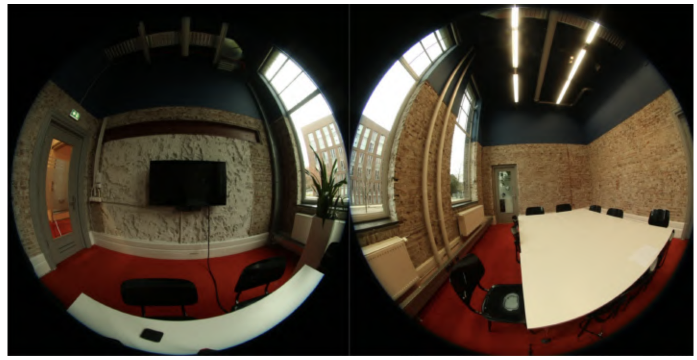

Fig. 1. The case study room

B. Material characterization scenarios

The following four methods for characterizing material optical properties are considered:

1) Manual selection from a material database: Material properties were manually selected based on color and type from *SpectralDB*.

2) Average Hemispherical Reflectance (AHR): Reflectance values for each sub-surface were calculated based on luminance and illuminance measurements, assuming the following relation:

$$\rho = \pi * (L/E) \tag{1}$$

where ρ is diffuse reflectance, L is luminance, and E is illuminance.
This method, known as Average Hemispherical Reflectance (AHR), is assumed as the ground truth method for material characterization in this study. Specularity and roughness values were assigned a value of zero.

3) Illuminance-proxy method: HDR images of five main surfaces, i.e. walls and ceiling, were captured. The validity of the resulting luminance map was tested against measured luminance values of three spots in the Field of View (FOV).
A list of sparse points of known reflectance values, measured with the AHR method, was created. A mask, indicating the area of interest in each HDR image was created as the third input of this method. In Fig. 3 these inputs for calculating the mean reflectance in one of the walls are visualized. Knowing the luminance and reflectance, an illuminance map is generated. The resulting list of illuminance values and their pixel location is then fed into a Kriging interpolation algorithm, as previously implemented by Mardaljevic et. al. [12]. The resulting illuminance map and the input luminance map are used to generate the reflectance map. Finally, the reflectance is calculated by averaging the pixel-wise reflectance values across the area of interest, indicated by the mask, e.g., brick parts, plinth (see Fig 3).
An additional outlier removal step, which includes the removal of 0-5$^{\text{th}}$ and 95-100$^{\text{th}}$ percentiles is applied to the list of output reflectance values for one of the surfaces (*wall 3*). This was only done on this wall because for other surfaces this did not significantly change the result (less than 5%).
A geometrically simplified model was also created by approximating a big surface, e.g. a wall, with many sub-surfaces, such as pipes and ducts, to a single polygonal surface. This is visualised for two example surfaces in Fig. 2.
Like the AHR method, specularity and roughness are assumed to be zero in this characterization scenario. For the definition of the floor, reflectance from the measurements is used for

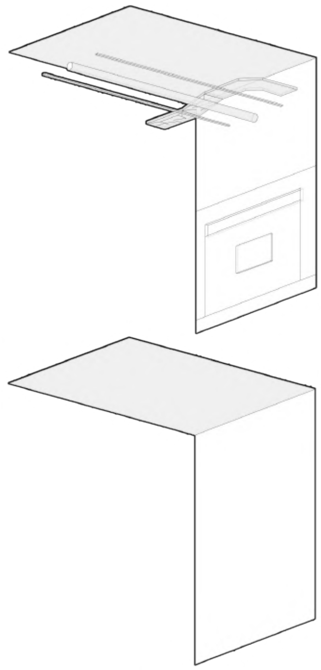

Fig. 2. Geometrical simplification adopted in the illuminance-proxy method.

simulation, since it was not possible to capture a full image of the floor.

4) Image-based probabilistic estimation: An Artificial Neural Networks model was constructed to quantitatively characterize material properties under random daylight conditions, consisting of an input layer with the shape of 128*128*3 (pixels*pixels*channels), one hidden layer, and an output layer with five neurons, for estimation of the following variables:

1) Reflectance in the red channel
2) Reflectance in the green channel
3) Reflectance in the blue channel
4) Specularity
5) Roughness

Mean squared error (MSE) was selected as the loss function to optimize the ANN model. Number of neurons was fine-tuned in from a search space of 1 to 400 neurons. 16 is shown to give the least loss (0.05). This neural network model was trained by a rendered data set with 1288 materials measured with a reflectance spectrophotometer [10](see Fig. 4). Each material was labeled with the above-mentioned information to define the material optical properties. The Radiance rendering engine [13] was used to generate a dataset of images of a flat surface perpendicular to the virtual camera for training. The rendered views were compressed from a four-channel HDR image to JPG images with three color channels to be read by the ANN model. A set of 16 random rendered samples are presented in Fig. 5.

The training data set is split into two training and validation sets with 1159 and 129 samples, respectively. Seven images of surface materials – including an exposed brick wall – from the studied room under random daylight illumination were cropped from images of the room to estimate the optical properties with the ANN model (see Fig. 6).

Fig. 5. Rendered samples for training the ANN.

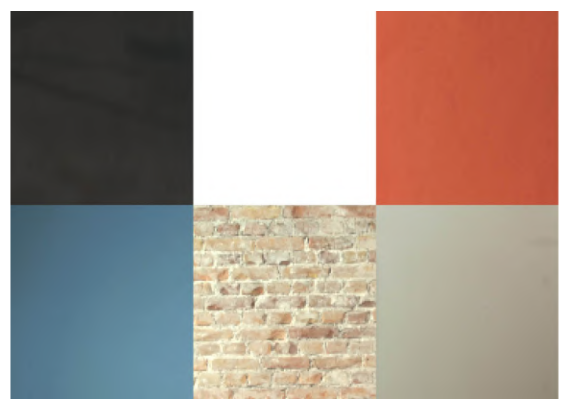

Fig. 6. Input samples of materials as real-world test cases. Top row from left to right: black screen, white desk, and orange floor. Bottom row from left to right: painted blue walls and ceiling, brick walls, opaque parts of the doors

C. Daylight performance simulation

The Radiance 2-phase method was chosen to run annual daylight simulations, using Honeybee [14] as the interface. Five daylight performance metrics are used in this study, including Daylight Autonomy (DA), continuous Daylight Autonomy (cDA), and three Useful Daylight Illuminance (UDI) values representing under-lit, well-lit, and over-lit areas. The thresholds for calculating these metrics are 300 lux for DA and UDI (lower threshold), and 3000 lux as the upper threshold for UDI.

The output of each material characterization scenario is applied on a single room described in section IV-A. Other information necessary for daylight calculations, including context and transmittance of windows, are maintained constant for all scenarios.

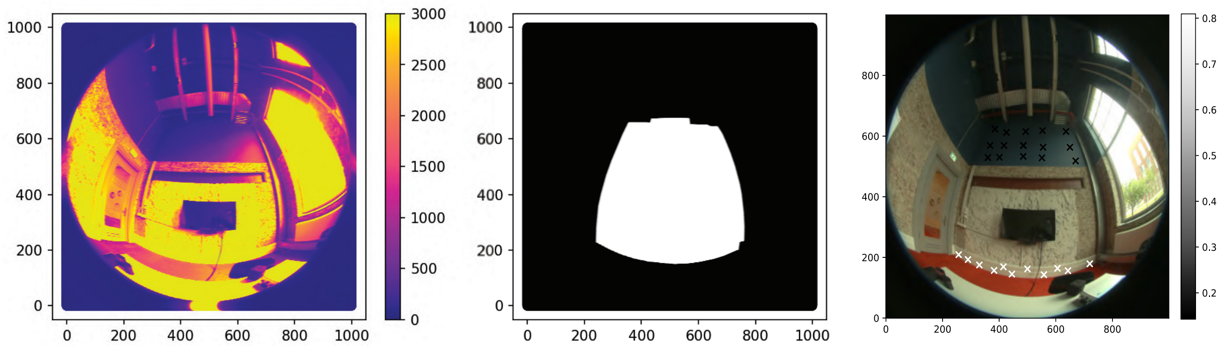

Fig. 3. Inputs for the illuminance-proxy method. From left to right: luminance map [cd/m^2], masked area, spots of known reflectance

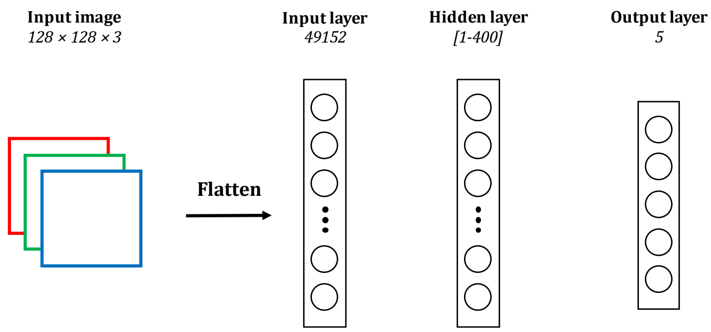

Fig. 4. Representation of the simple ANN used in this study.

V. Results

Firstly, the results from the various material characterisation methods are presented and compared against the AHR method. Secondly, the corresponding daylight simulation results are presented.

A. Material properties

The visible reflectance values given by the AHR, SpectralDB (manual selection), illuminance proxy, and ANN methods are presented in Fig. 7. Since specularity is assumed to be zero in AHR and illuminance proxy, only the estimation of specularity resulting from ANN and SpectralDB are presented in Fig. 8. The results show that SpectralDB predicts reflectance more accurately compared to ANN, however, this prediction resulted in significant error in characterizing the reflectance of *White desk*, *Floor*, *Windows sill*, and *Flower box*. Reflectance results from the illuminance-proxy method gives the reflectance for *brick* and *plaster*, as well as the minor sub-surfaces including *black screen* and *red beam* with less than 5% absolute error. Errors are considerable for *white pipes*, *silver ducts*, and *radiators*. The results for radiators is above 1, even with outlier removal.

The output illuminance map, reflectance map, and the final mean reflectance values from the illuminance-proxy method corresponding to the model with geometrical simplification, for five surfaces including four walls and the ceiling, are presented in Table I. These mean values range from 0.36 for the ceiling to 0.481 for *wall1*. As mentioned in Section IV-B3, for *wall3* the initial mean reflectance output was 1.48, so an outlier removal was applied (removal of lowest and highest five percentiles), and the resulting value, 0.42, is considered for the daylight simulation.

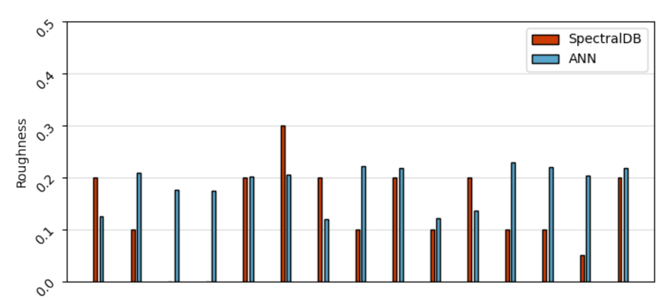

Fig. 8. Comparison of specularity values from ANN and SpectralDB

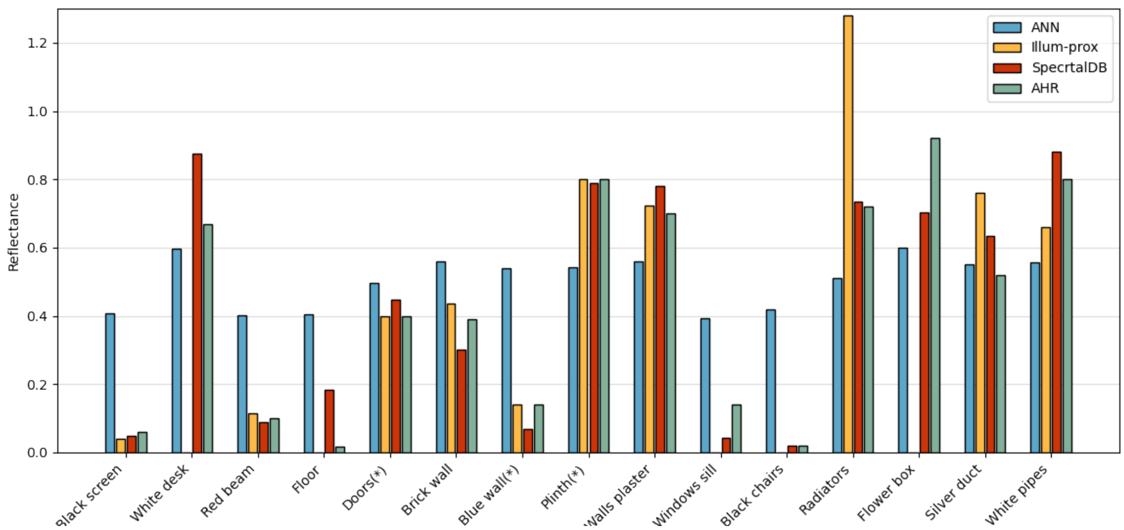

Fig. 7. Visible reflectance values from AHR, SpectralDB, illuminance proxy, and ANN. Reflectance values corresponding to the surfaces indicated by (*) are include the spots with known reflectance as the input for illuminance-proxy methods, thus are equal to AHR.

B. *Annual daylight performance metrics*

The spatially averaged performance values corresponding to each of the four material characterization scenarios are presented in Fig. 9. A more detailed comparison was done to capture the deviation of each annual performance metric from the AHR scenario across all the points on the simulation grid. The RMSE values resulting from this comparison are presented in Fig. 10.

According to the daylight results in Fig. 9, the performance metrics from the illuminance proxy method with and without geometrical simplification falls within 5% error range for DA, cDA, and $UDI_{\text{well-lit}}$ and it predicts $UDI_{\text{over-lit}}$ with less than 10% error. Nevertheless, the error in calculation of $UDI_{\text{under-lit}}$ is more than 15%.

Comparing the annual results across grid points (Fig. 10) shows that, while illuminance proxy results agrees the most with the ground truth model, geometrical simplification causes significant errors in predicting $UDI_{\text{under-lit}}$ and $UDI_{\text{well-lit}}$, and while performing almost similarly with ANN in calculating cDA, it is considerably more accurate than ANN overall.

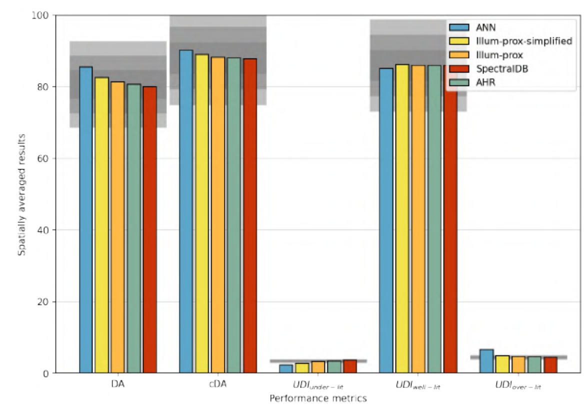

Fig. 9. Average values of annual daylight performance metrics with 5, 10, and 15% error range relative to AHR

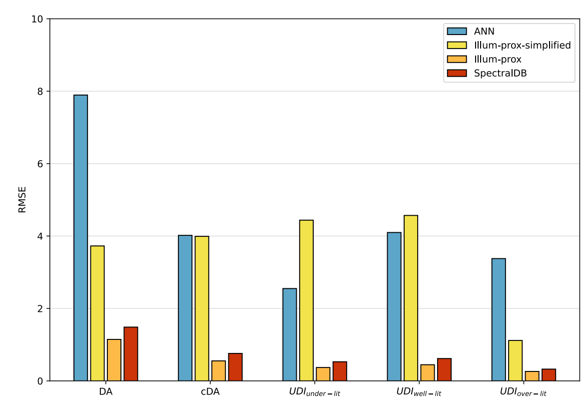

Fig. 10. Root Mean squared error (RMSE) of annual performance values across the simulation grid range relative to AHR

VI. Discussion

Annual daylight results (Fig. 9 and 10) indicate that illuminance-proxy performs better that the other methods, showing less than 10% error relative to the model corresponding to AHR technique. However, significant errors exist when geometrical simplification is applied.SpectralDB also shows good agreement with the ground truth, however, significant errors exist when this comparison is done for visible reflectance values as shown in Fig. 7.Such errors are more than 10% for a few surfaces, namely *White desk*, *Floor*, *Plinth*, *Walls-plaster*, *Windows-sill*, and *Flower box*.

TABLE I

INTERPOLATED ILLUMINANCE MAP, REFLECTANCE MAP, AND MEAN REFLECTANCE FOR FIVE MAIN SURFACES OF THE STUDIED ROOM

Surface name	Input HDR map [cd/m^2]	Illuminance map[lx]	Reflectance map[0-1]	Mean reflectance
Wall1	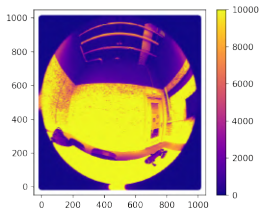	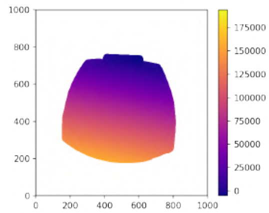	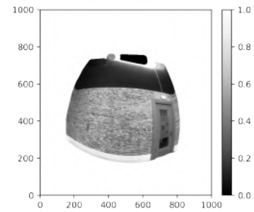	0.481
Wall2	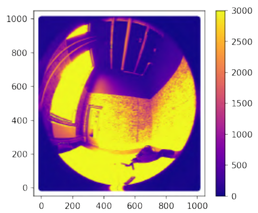	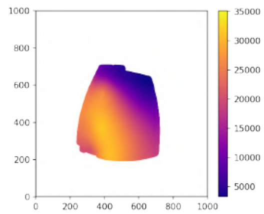	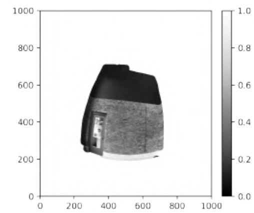	0.361
Wall3	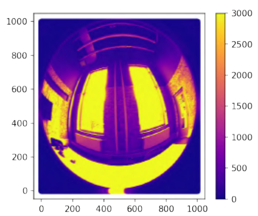	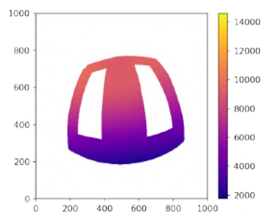	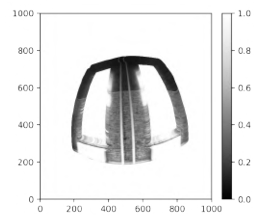	0.42
Wall4	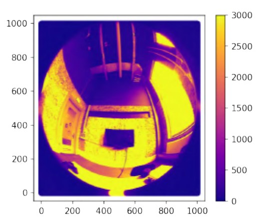	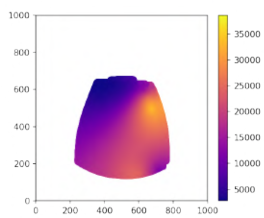	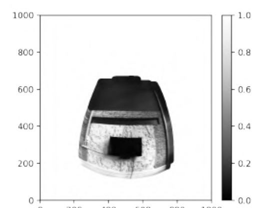	0.44
Ceiling	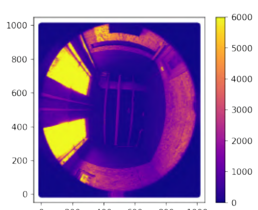	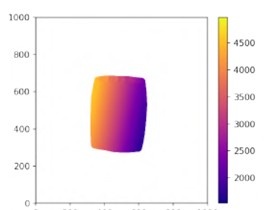	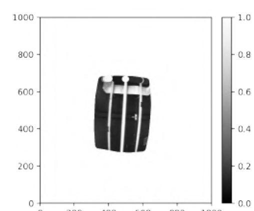	0.36

There are three underlying assumptions in the illuminance-proxy method:

1) The area of interest does not have significant protrusions and is flat.
2) The light that falls onto each surface has smooth illuminance variations.
3) All of the surfaces and materials in the FOV are diffuse.

Any geometrical and lighting conditions deviating from these assumptions will cause error in the final results. A possible source of errors in many cases is the existence of specular surfaces, resulting in over-prediction of average reflectance, and consequently, daylight results. This over-prediction has been significant for two specular surfaces, namely *silver ducts*, *radiators* (see Fig. 7) and *wall3*(see Section IV-B3). This outliers might also be partly caused by abrupt changes in the illuminance levels on the areas close to the windows, which can be the result of inaccurate masking of the opening areas. According to annual average results, ANN has less than 5% error in the calculation of DA, cDA, $UDI_{under\text{-}lit}$ (Fig.9).

Fig. 11. Rendered scene corresponding to each measurement scenario, from left to right: (1) AHR, (2)SpectralDB, (3)Illuminance-proxy, (4) Illuminance proxy with geometrical simplification,and (5)ANN

However, except for *White desk*, *Doors*, *Walls-plaster*, and *Silver duct*, it estimated the visible reflectance with significant error. The predicted specularity results are not realistic, while seven (out of fifteen) predictions for roughness are close to those suggested by SpectralDB for a similar material (Fig. 8). Five renderings of the room (Fig. 11), corresponding to each scenario reveals the inaccurate predictions of ANN.

Inaccurate predictions of ANN is also confirmed by analysing hourly illuminance values for all the grid points with RMSE of31.62 for illuminance-proxy, 98.52 for illuminance proxy(simplified), 44.02 for SpectralDB, and 270.75 for ANN.

VII. Conclusion

In this study, four material characterization scenarios are implemented to define material properties of opaque surfaces in a single meeting room. Accuracy of these methods are evaluated both by comparing the reflectance values, and by annual daylight provision metrics. Illuminance-proxy has shown promising results for pixel-wise reflectance characterization and proved to be a powerful alternative for manual point-by-point measurements of luminance and illuminance (AHR) as a common approach. Nevertheless, this method is prone to error specially when a specular surface is in the FOV. Manual selection of materials from SpectralDB has also shown to give accurate results compared to ANN. Still, all the scenarios showed acceptable results in predicting average annual performance metrics, i.e., DA, cDA, and $UDI_{\text{well-lit}}$ with less than 5% error, while significant error exists in calculation of material properties, namely reflectance and specularity. Both methods have potentials in digitizing the process of daylight modeling. Illuminance proxy reduces the measurement costs by reducing the number of AHR and offers pixel-wise material reflectance map of areas within the FOV. This is a good solution for complex surfaces.

This project is limited in some aspects, which will be described in the next paragraphs. Future research will address these limitations.

- *Reliable ground truth measurement.* Average Hemispherical Reflectance (AHR) technique is used as the ground truth value for visible reflectance in this study. Since this method does not capture detailed information regarding the five key optical properties, a similar material from a measured data set (SpectralDB) is used to check the validity of the ANN outputs for specularity and roughness (see Fig. 8). Even in that data set, the roughness values assigned to each material are not coming from accurate measurements and are based on a rule of thumb introduced by Jones and Reinhart [15]. A more reliable data measured in the studied space is needed to check the validity of the outcomes. This can be done using reflectance spectrophotometers [16].
- *Error measurement for illuminance proxy.* In this study, daylight results were used to quantify the errors associated with the uncertainties in the illuminance proxy method (see Section VI). To do this task more reliably, a predicted mean reflectance should be calculated based on accurate measurements.
- *Improved learning approaches.* In this study a simple neural network, consisting of one hidden layer with 16 neurons, with linear activation is used. This simple architecture does not capture the capabilities of probabilistic methods. In future research, this will be addressed by generating other training datasets under a certain lighting condition, which is reproducible in the indoor space. This will be done to reduce the uncertainties concerning the lighting conditions. Furthermore, other learning architectures proven to perform well on material classification task will be adapted to the problem of this research [17, 18]. Lastly, based on the reliable results from manual selection of materials (SpectralDB), approaching the learning-based material characterization as a classification, rather than regression (as done in this study) might give more accurate results and will be further developed in the future studies.

VIII. Acknowledgement

We thank Dr. Stef Lhermitte for useful discussions.

References

[1] Ann R. Webb. “Considerations for lighting in the built environment: Non-visual effects of light”. In: *Energy and Buildings* 38.7 (July 2006), pp. 721–727. ISSN: 03787788. DOI: 10.1016/J.ENBUILD.2006.03.004.

[2] *EU Buildings Database*. URL: https://ec.europa.eu/energy/eu-buildings-database_en (visited on 01/17/2022).

[3] Eleonora Brembilla, Christina J Hopfe, and John Mardaljevic. “Influence of input reflectance values on climate-based daylight metrics using sensitivity analysis”. In: *Journal of Building Performance Simulation* 11.3 (2018), pp. 333–349.

[4] John Mardaljevic, Eleonora Brembilla, and Nafsika Drosou. “Illuminance-proxy high dynamic range imaging: a simple method to measure surface reflectance”. In: (2015).

[5] Nafsika Drosou and John Mardaljevic. *Real World Complexity in Reflectance Value Measurement for Climate-Based Daylight Modelling - Data*. 2016. DOI: 10.17028/rd.lboro.3364747.v2.

[6] Sean Bell et al. “Material Recognition in the Wild with the Materials in Context Database”. In: *Proceedings of the IEEE Computer Society Conference on Computer Vision and Pattern Recognition* 07-12-June (Dec. 2014), pp. 3479–3487. ISSN: 10636919. DOI: 10.48550/arxiv.1412.0623. arXiv: 1412.0623. URL: https://arxiv.org/abs/1412.0623v2.

[7] *OpenSurfaces - A Richly Annotated Catalog of Surface Appearance*. URL: http://opensurfaces.cs.cornell.edu/ (visited on 05/04/2022).

[8] Michael Weinmann, Juergen Gall, and Reinhard Klein. “Material Classification Based on Training Data Synthesized Using a BTF Database”. In: *Lecture Notes in Computer Science (including subseries Lecture Notes in Artificial Intelligence and Lecture Notes in Bioinformatics)* 8691 LNCS.PART 3 (2014), pp. 156–171. ISSN: 16113349. DOI: 10.1007/978-3-319-10578-9_11. URL: https://link.springer.com/chapter/10.1007/978-3-319-10578-9_11.

[9] B Andres et al. “Vision, Modeling, and Visualization (2021) Capturing Anisotropic SVBRDFs”. In: (2021). DOI: 10.2312/vmv.20211372. URL: https://diglib.eg.org.

[10] Alstan Jakubiec. *Spectral Materials Database*. URL: http://spectraldb.com/ (visited on 03/28/2022).

[11] Rabia Rashdi et al. “Scanning Technologies to Building Information Modelling: A Review”. In: *Infrastructures* 7.4 (2022), p. 49.

[12] John Mardaljevic et al. “A hybrid measurement-simulation approach to determine the reflectance map of a historic tapestry”. In: *Building Simulation 2021 Conference: BS2021*. International Building Performance Simulation Association. 2021.

[13] Gregory J Ward. “The RADIANCE lighting simulation and rendering system”. In: *Proceedings of the 21st annual conference on Computer graphics and interactive techniques*. 1994, pp. 459–472.

[14] Mostapha Sadeghipour Roudsari, Michelle Pak, Adrian Smith, et al. “Ladybug: a parametric environmental plugin for grasshopper to help designers create an environmentally-conscious design”. In: *Proceedings of the 13th international IBPSA conference held in Lyon, France Aug*. 2013, pp. 3128–3135.

[15] Nathaniel L Jones and Christoph F Reinhart. “Experimental validation of ray tracing as a means of image-based visual discomfort prediction”. In: *Building and Environment* 113 (2017), pp. 131–150.

[16] Greg Ward and Rob Shakespeare. *Rendering with Radiance: the art and science of lighting visualization, Chapter 5*. Randolph M.Fritz, 1998.

[17] Hanxiao Liu et al. *Hierarchical Representations for Efficient Architecture Search*. 2017. DOI: 10.48550/ARXIV.1711.00436. URL: https://arxiv.org/abs/1711.00436.

[18] Adrian de Wynter. “On the Bounds of Function Approximations”. In: *Artificial Neural Networks and Machine Learning – ICANN 2019: Theoretical Neural Computation*. Springer International Publishing, 2019, pp. 401–417. DOI: 10.1007/978-3-030-30487-4_32. URL: https://doi.org/10.1007%2F978-3-030-30487-4_32.